A Closed-Form Analytical Estimation of Vertical Displacement Error in Pedestrian Navigation

Chi-Shih Jao, Yusheng Wang, Sina Askari, and Andrei M. Shkel
Microsystems Lab, University of California, Irvine, CA, USA
Email: {chishihj, yushengw, askaris, ashkel}@uci.edu

***Abstract*—We present an analytical expression for estimating the position error in the vertical direction in pedestrian navigation using an Inertial Measurement Unit (IMU) aided by an altimeter. The analytical expression is found to be directly proportional to the altimeter resolution, the square root of the altimeter sampling rate, IMU Velocity Random Walk (VRW), and a ratio of time intervals in the stance phase and the swing phase during the gait cycle, and inversely proportional to the square root of IMU sampling rate. The analytical analysis was verified by numerical simulations and supported by experimental results. The numerical simulation of the ZUPT-augmented navigation aided by an altimeter was conducted based on a mathematically simulated foot motion trajectory. Experiments were implemented on a foot-mounted platform containing IMUs and altimeters. The results from both simulations and experiments matched our analytical prediction, with an error less than 20%.**

***Index Terms*—Sensor Fusion, Inertial Navigation Systems, Altimeter, Pedestrian Navigation**

I. Introduction

The Inertial Navigation Systems (INS) based on Micro-Electro-Mechanical Systems (MEMS) have a variety of applications for small platforms and pedestrians, and have been considered for augmentation of GPS, Signals of Opportunity, and self-contained navigation solutions when GPS or signals of opportunity are not available [1], [2]. The INS utilizes acceleration and angular velocity sensors from the Inertial Measurement Unit (IMU), and calculates the position, orientation, and velocity of an object by dead reckoning [3]. However, Commercial Off-The-Shelf (COTS) MEMS-based IMUs still suffer from a high noise level, which leads to drift in estimation of an object's position [4], especially when used as self-contained navigation solutions. Therefore, calibration methods and multi-sensor fusion solutions are beneficial to consider.

One effective velocity calibration method in a pedestrian INS is Zero velocity UPdaTe (ZUPT) [5]. Such a method uses shoe-mounted IMUs of a pedestrian and considers as the ground truth the event when the foot's velocity is very close to zero during the stance phase of the walking gait cycle [6]. The algorithm uses this information to update states in an Extended Kalman Filter (EKF) framework. With a proper setting of the ZUPT threshold, this approach allows to achieve an accuracy of 1 meter after traveling on the order of 100 meters [7]. However, the displacement drifts are still significant for a long-term navigation when navigation algorithms are based solely on the ZUPT.

To further improve the navigation accuracy of a ZUPT-augmented INS, measurements obtained from additional sensors can be synthesized in the system by multi-sensor fusion. Pressure-based altimeters are popular devices for this purpose as they provide independent and direct measurements of position along the vertical direction. Barometer/altimeter data for INS has been shown to improve the overall navigation results in various types of integrated INS [8]–[13]. One type of INS has adopted a foot-mounted low-cost IMU and combined ZUPT, altimeter, and magnetometer measurements in the EKF framework [13] to study the IMU bias impact on the performance of foot-mounted INS.

Pedestrian INS can be designed to perform numerous tasks, which have different criteria for navigation accuracy. When it comes to designing an integrated INS for pedestrian navigation, the size, weight, power, and cost (SWaP+C) budget would affect the performances of the sensors of choice, and a trade-off between SWaP+C and navigation accuracy has to be considered. The analytical estimations of velocity errors in the north, east, and down directions were previously derived in [14] and the position error standard deviations in the north and east directions were analytically estimated in [15] for a ZUPT-augmented INS. These estimations also apply to the case of a ZUPT/altimeter-aided INS because the altimeter measurements have a distinct effect on positions in the down direction, but affect negligibly the other states. This paper focuses on a closed-form analytical estimation of the displacement error in the down (vertical) direction in a ZUPT/altimeter-aided INS.

The three main contributions of the paper are: 1) It directly relates the displacement error in the down direction to altimeter resolution and its sampling rate, IMU VRW and its sampling rate, and the swing phase and the stance phase percentage of the gait cycle. 2) It validates the analytical estimation of the displacement error standard deviation in the down direction using simulated IMU and altimeter measurements. 3) It validates the derived analytical estimation experimentally using real IMU and altimeter measurements, implementing a ZUPT/altimeter aided INS using EKF.

This paper is organized as follows. In section II, we briefly present an implementation of the strapdown navigation aided

This work is performed under the following financial assistance award: 70NANB17H192 from US department of Commerce, National Institution of Standards and Technology (NIST).

978-1-7281-0244-3/20/$31.00 ©2020 IEEE

Authorized licensed use limited to: Access paid by The UC Irvine Libraries. Downloaded on June 12,2020 at 03:58:13 UTC from IEEE Xplore. Restrictions apply.

by ZUPT and altimeter measurements in an EKF framework, and then analytically derive the displacement estimation error in the down direction. In section III, we verify the closed-form analytical expression by simulated and experimental IMU and altimeter measurements.

II. Aided Inertial Navigation

In this section, we first present how the ZUPT and altimeter measurements are incorporated in the EKF with a standard strap-down navigation algorithm. Next, we present an error analysis to estimate a lower bound of the error covariance displacement along the down direction and discuss what parameters would affect the navigation accuracy.

A. Strapdown Inertial Navigation with EKF

We implement a standard strap-down inertial navigation system in the navigation frame [3]. The output from the INS is corrected in the EKF by keeping track of the states $\delta x = [\delta\theta_n^T, \delta v_n^T, \delta s_n^T]$, where $\delta\theta_n$, δv_n, and δs_n are the altitude, velocity, and position errors along the north, east, and down directions of the navigation coordinate frame [3].

The dynamic model of EKF is approximated as follows:

$$\begin{aligned}\delta\dot{x} &= \begin{bmatrix} 0_{3\times3} & 0_{3\times3} & 0_{3\times3} \\ [\overrightarrow{f}^n\times] & 0_{3\times3} & 0_{3\times3} \\ 0_{3\times3} & I_{3\times3} & 0_{3\times3} \end{bmatrix}\delta x + \begin{bmatrix} C_b^n ARW \\ C_b^n VRW \\ 0_{3\times1} \end{bmatrix} \\ &\triangleq A(t)\delta x + B(t),\end{aligned}$$

where $[\overrightarrow{f}^n\times]$ is the skew-symmetric cross-product-operator of the accelerometer output in the navigation frame; ARW is Angle Random Walk of the gyroscopes; VRW is the Velocity Random Walk of the accelerometers, and C_b^n is the Directional Cosine Matrix (DCM) from the navigation frame to the body frame. $A(t)$ and $B(t)$ are time varying matrices.

This continuous-time model is discretized by the Euler's Equation since the sampling period Δt of the IMU is small, and the dynamic matrix can be expressed as

$$\begin{aligned}F_k &= exp(A(t_k)\Delta t) \approx I + A(t_k)\Delta t, \\ B_k &= B(t_k)\Delta t, \\ Q_k &= diag(B_k)\Delta t.\end{aligned}$$

The EKF prediction equations are

$$\begin{aligned}\delta\bar{x}(k+1) &= F_k\delta x(k), \\ \bar{P}(k+1) &= F_k P(k) F_k^T + Q_k,\end{aligned}$$

where $\delta\bar{x}(k+1)$ is the predicted states and $\bar{P}(k+1)$ is the *a priori* covariance matrix at the $(k+1)^{th}$ step.

On the updated step, we use both altimeter and ZUPT to correct the INS output. The altimeter measurement updates the system states when a measurement is available, and the ZUPT comes in when a stance phase is detected. Pressure-based altimeters measure the absolute air pressure p, which can be converted to the displacement along the down direction x_D [11] by the equation

$$x_D = 443300 \times \left(1 - \left(\frac{p}{p_0}\right)^{\frac{1}{5.255}}\right),$$

where p_0 is the absolute pressure at the sea level. For the ZUPT algorithm, we use a mechanism such that a stance phase is detected when the summation of variances of gyroscope readout g_{VAR} and that of accelerometer readout a_{VAR} are lower than a specified threshold γ. It can be described as

$$ZUPT\ status = H\left(\frac{a_{VAR}}{\sigma_a} + \frac{g_{VAR}}{\sigma_g} - \gamma\right),$$

where H() is a Heaviside function, σ_g and σ_a are normalized amplitudes of VRW and ARW.

The measurement equation of the EKF has different forms for each of the following three cases: 1) A stance phase is detected (ZUPT ON) and the altimeter has a null measurement, 2) A swing phase is detected and the altimeter acquires a measurement (altimeter ON), and 3) A stance phase is detected and the altimeter obtains a measurement (Both ON). Note that the altimeter can provide null measurement. For example, we use an IMU with $100Hz$ sampling rate and an altimeter with $10Hz$ sampling rate. The altimeter acquires an effective measurement at the first IMU sample. Then in the following 9 IMU samples, we consider that the altimeter gives null measurement. The measurement equation of the EKF is expressed as follows:

$$z = Hdx(k) + \omega_k,$$

where

$$\begin{cases} z = \begin{bmatrix} \delta v_N \\ \delta v_E \\ \delta v_D \end{bmatrix}, & \text{if } ZUPT\ ON \\ H = \begin{bmatrix} 0_{3\times3} & I_{3\times3} & 0_{3\times3} \end{bmatrix}, & \\ \\ z = \begin{bmatrix} \delta x_D \end{bmatrix}, & \\ H = \begin{bmatrix} 0_{1\times3} & 0_{1\times3} & [0\ 0\ 1] \end{bmatrix}, & \text{if } altimeter\ ON \\ \\ z = \begin{bmatrix} \delta v_N \\ \delta v_E \\ \delta v_D \\ \delta x_D \end{bmatrix}, & \text{if } Both\ ON \\ H = \begin{bmatrix} 0_{3\times3} & I_{3\times3} & 0_{3\times3} \\ 0_{1\times3} & 0_{1\times3} & [0\ 0\ 1] \end{bmatrix}, & \end{cases}$$

where $dx(k)$ is the error state vectors, and ω_k, modeled as Gaussian distribution, is the measurement noises contributed from both the ZUPT and the altimeter. The ZUPT measurement noise comes from the velocity estimation error accumulated during the stance phase [16]. Note that in the last row of the H matrix, the location of 1 corresponds to a displacement along the down direction.

Authorized licensed use limited to: Access paid by The UC Irvine Libraries. Downloaded on June 12,2020 at 03:58:13 UTC from IEEE Xplore. Restrictions apply.

The EKF update equations are described as follows.

$$K = \bar{P}(k+1)H^T(H\bar{P}(k+1)H^T + R)^{-1},$$
$$v(k+1) = z - H\delta\bar{x}(k),$$
$$\delta x(k+1) = \delta\bar{x}(k+1) + Kv(k+1),$$
$$P(k+1) = (I - KH)\bar{P}(k+1),$$

where K is the Kalman gain, $v(k+1)$ is the innovation sequence, $\delta x(k+1)$ is the *a posteriori* state, and $P(k+1)$ is the covariance matrix at the $(k+1)^{th}$ step.

B. Estimation of error covariance in the down direction

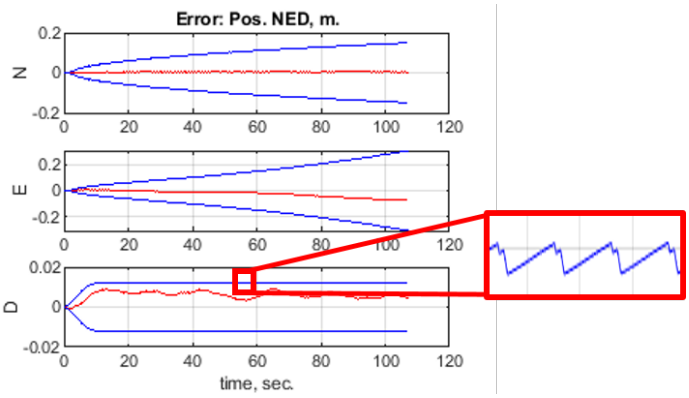

Fig. 1. A typical propagation of errors in displacement estimations in the INS aided by ZUPT and altimeter. N, E, and D are the displacements along the north, east, and down directions, respectively. The red curve in each plot is the error profile, and the blue curve indicates the 3σ limit of errors.

The analytical estimation of the displacement error in the down direction was motivated by an observation that the altimeter measurements are able to reduce the navigation error by restricting the error growth of displacement along the down direction. A typical propagation of errors in displacements along the north, the east, and the down directions and their covariances are presented in Fig. 1. We observed that while covariances of the errors in displacement estimation of the north and the east directions keep growing over time, the covariance along the down direction reaches a stable level with a small range of fluctuation. The fluctuation of the covariance follows a pattern that is reduced when measurements from an altimeter are acquired, and it increases when the measurements from the altimeter are not available. This observation inspired us to combine the altimeter parameters that determine the altimeter performance and the IMU parameters that are dominated in the free navigation. The combination enables us to fully analyze the system behavior and extract the covariance of the errors in the system's state estimation.

Since there are 15 states in the EKF implementation, the covariance matrix is 15×15. We divide the matrix into nine 3×3 sub-matrices. Each sub-matrix is indicated by a sub-index.

From the EKF propagation equations,

$$P_{22}^{priori}(3,3) = P_{22}(3,3) + (2P_{21}(3,2)a_N + VRW^2)\Delta t$$
$$= P_{22}(3,3) + 2P_{21}(3,2)v_N(t) + VRW^2 dt$$

Since the term with $P_{21}(3,2) \ll VRW^2$, an increase in $P_{22}(3,3)$ during the prediction step can be approximated as

$$\Delta_{pred}P_{22}(3,3) = VRW^2 dt$$

From the update step,

$$P_{22}^{posteriori}(3,3) = P_{22}^{priori}(3,3) - \frac{P_{22}^{priori}(3,3)^2}{\omega^2}$$

Consequently, the decrease in $P_{22}(3,3)$ during the update step is

$$\Delta_{update}P_{22}(3,3) = -\frac{P_{22}^{priori}(3,3)^2}{\omega^2}$$

Because the ZUPT algorithm limits the error covariance growth in velocities, the increase of $P_{22}(3,3)$ during the prediction step is equal to decrease in the update step,

$$\int_{t_{stride}} \Delta_{pred}P_{22}(3,3)dt = -\int_{t_{stance}} \Delta_{update}P_{22}(3,3)dt, \quad (1)$$

where t_{stride} is a time duration of the swing phase in a gait cycle, N_{stance} is a number of samples being updated by the ZUPT algorithm, and dt is a sampling rate of IMU. Rearranging (1), the covariance of the velocity along the down direction is

$$P_{22}(3,3) = \sqrt{\frac{VRW^2 t_{stride}\omega^2}{N_{stance}}}$$

To find $P_{23}(3,3)$, we start from the propagation equation,

$$P_{23}^{prior}(3,3) = P_{23}^{posteria}(3,3) + (P_{22}(3,3) + \alpha_N P_{13}(2,3))\Delta t$$

Since the term with $P_{13}(2,3)$ is much smaller than the term with $P_{22}(3,3)$, we can rewrite the equation and approximate the increase of $P_{23}(3,3)$ during the swing phase as,

$$\Delta_{pred}P_{23}(3,3) = P_{22}(3,3)dt = \sqrt{\frac{VRW^2 t_{stride}\omega^2}{N_{stance}}}dt$$

After taking the integral, equation (1), from 0 to t, we obtain

$$P_{23}(3,3) = \sqrt{\frac{VRW^2 t_{stride}\omega^2}{N_{stance}}}t$$

Now, we are ready to derive $P_{33}(3,3)$. From the propagation equation, the increase of displacement covariance along the down direction, when the altimeter measurement is not available, is

$$\Delta_{pred}P_{33}(3,3) = P_{33}^{prior}(3,3) - P_{33}^{posteria}(3,3)$$
$$\approx (2P_{23}(3,3))\Delta t$$

From the update equation discussed in section II-A, the decrease in covariance when altimeter data is obtained is

$$\Delta_{update}P_{33}(3,3) = P_{33}^{posteria}(3,3) - P_{33}^{prior}(3,3)$$
$$= -\frac{P_{23}(3,3)^2}{\omega^2} - \frac{P_{33}(3,3)^2}{alt^2},$$

where alt is the altimeter measurement noise, which is identical to the altimeter resolution.

Authorized licensed use limited to: Access paid by The UC Irvine Libraries. Downloaded on June 12,2020 at 03:58:13 UTC from IEEE Xplore. Restrictions apply.

Since the displacement covariance along the down direction is bounded by altimeter measurements,

$$\int_{t_{ALT\ OFF}} \Delta_{pred} P_{33}(3,3) = -\int_{t_{ALT\ ON}} \Delta_{update} P_{33}(3,3), \tag{2}$$

where $t_{ALT\ ON}$ is the total amount of time that the altimeter is obtaining data within a gait cycle, and $t_{ALT\ OFF}$ is the rest of the time in the gait cycle. Taking the integration, the estimate of the error covariance of displacement along the down direction is

$$P_{33}(3,3) = (\sqrt{\frac{VRW^2 t_{stride}\omega^2}{N_{stance}}}\frac{t_{ALT\ OFF}}{N_{ALT\ ON}} - \frac{VRW^2 t_{stride}}{3N_{ALT\ ON}} N_{stance} t_{ALT\ ON})^{\frac{1}{2}} \frac{alt}{\sqrt{dt}}.$$

A few observations can be made from the analytical solution:

1) The variance of the vertical displacement estimate in the EKF is affected by VRW, but is independent of ARW.
2) Altimeter sampling rate and resolution are key factors in estimation of variance.
3) The ratio of the swing phase and the stance phase during the gait cycle would affect the estimate of variance.

III. Simulation and Experiment

Two sets of numerical simulations and experiments were conducted to verify the derived analytical expression. In this section, we present how the simulations and experiments were conducted and discuss their results.

In the first set of simulations and experiments, we looked into the effect of altimeter resolution on displacement error along the down direction. For simulation, a trajectory of foot toward north and the corresponding IMU and altimeter readouts were generated based on a human gait analysis [14]. The stride length was set to 0.6 [m], and each step was considered identical. VRW of the IMU was set to 0.023 $mg/\sqrt{Hz}$, and ARW to 0.3 $\deg/\sqrt{h}$. The altimeter sampling rate was set to 20 Hz. The total navigation time was 107s. Then, different levels of altimeter noises, from 10^{-3} [m] to 10 [m], were added to the readouts. Next, the ZUPT-augmented inertial navigation algorithm aided by altimeter was applied to the IMU and altimeter readouts. A flexible laboratory testbed [17] was used to perform the experiments. We considered five additional pressure-based altimeters, MS-5803-01BA, MS-5803-02BA, MS-5803-05BA, MS-5803-14BA, and MS-5803-30BA. We then experimentally determined their resolutions, which were found to be 0.29 [m], 0.6 [m], 1.5 [m], 5 [m], and 10 [m], respectively. For each altimeter, we conducted a set of 6 similar experiments. In each experiment, the total navigation time was 90 [sec].

Fig. 3 shows a relation between altimeter resolution to the estimated position error's standard deviation along the down direction. The blue curve corresponds to the analytical estimation of the error displacement covariance; the red circles

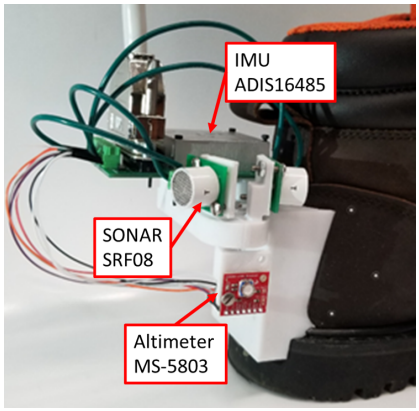

Fig. 2. Illustrated is a test platform integrated with an MS-5803 altimeter.

indicate the results of the simulation, and the blue solid triangles represent the statistical means of the results from the 6 experiments using the same altimeter. The results show that the analytical and the simulation estimates were closely matched within 15% for altimeter resolutions higher than 0.05m. This mismatch came mainly from omitting the terms that have relatively small values in the derivation of the analytical estimates. For the case of lower altimeter resolutions, the term with $P_{13}(2,3)$ was no longer 10 times smaller than $P_{33}(3,3)$, and a larger discrepancy percentage was expected. Fig. 3 also shows a difference within 16% between the analytical estimation and experimental results. The discrepancy between the analytical estimation and experimental results was contributed not only by omission of the small-value terms but also by the following two factors: 1) foot dynamics considered in the derivation was not exactly the same as the actual walking experiments and 2) the altimeter measurements could be affected by abrupt changes in air pressure during the experiments.

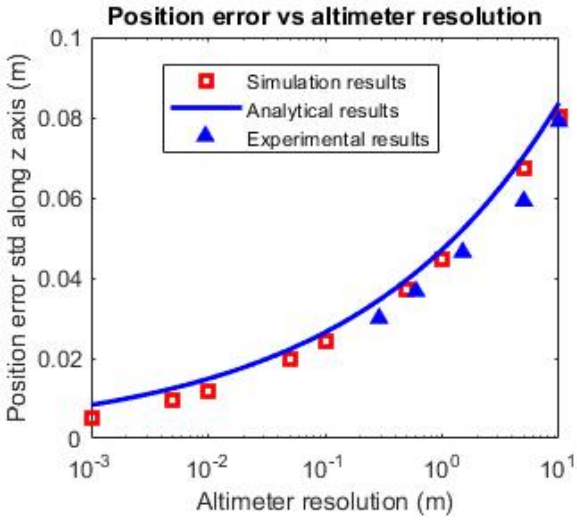

Fig. 3. The relation of altimeter resolution and the displacement error standard deviation along the down direction.

In the second set of simulation and experiment, we inves-

Authorized licensed use limited to: Access paid by The UC Irvine Libraries. Downloaded on June 12,2020 at 03:58:13 UTC from IEEE Xplore. Restrictions apply.

tigated a relationship between the altimeter sampling rate and the displacement covariance. The simulation setup was the same as in the first set, except that in this case, the altimeter resolution was set to 0.1 [m] and its sampling rate was swept from 2 to 100Hz. In the experiment, the altimeter MS-5803-01BA was used with our custom navigation platform, and the sampling rate was swept from 1 to 20Hz. Nominal trajectories were the same as in the first experiment, and 6 experiments were conducted for each sampling rate.

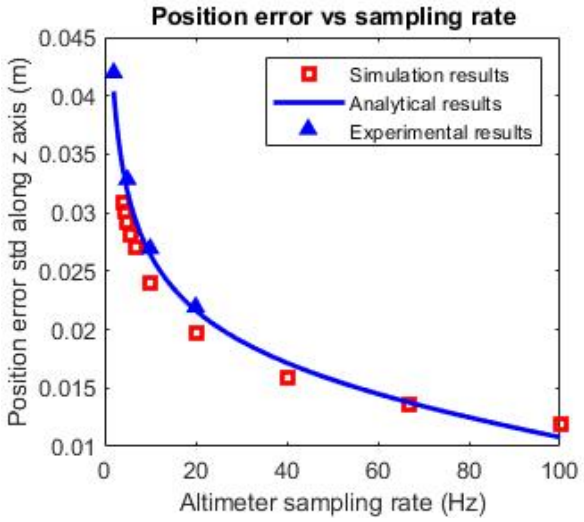

Fig. 4. The relation of altimeter sampling rate and the displacement error standard deviation along the down direction.

Fig. 4 shows the effect of altimeter sampling rate on the estimated position error standard deviation along the down direction. The blue curve corresponds to the analytical estimation of the error displacement covariance; the red circles indicate the results of the simulation, and the blue solid triangles represent statistical means of the results from the 6 experiments using the same altimeter. The results show that the numerical simulation results differed from the analytical results by less than 20%. We can see that the discrepancy between them tended to increase as the altimeter sampling rate was increased. This was anticipated because an increase in the altimeter sampling rate led to a longer integration intervals for the second integral in equation (2), in which we neglected the term $P_{21}(3,2)$ because of the assumption $P_{21}(3,2) << VRW^2$. The difference between experimental results and analytical results was within 5%. Note that we only showed altimeter sampling rates lower than $20Hz$ due to the limitation of the sampling rate of altimeter MS-5308 in data acquisition communication protocol.

IV. Conclusion

In the paper, we derived an analytical solution for position variance estimation in the case of inertial navigation aided by ZUPT and altimeter measurements. The solution showed that the displacement error variance along the down direction was directly related to the altimeter resolution, altimeter sampling rate, IMU VRW, IMU sampling rate, and the swing phase and the stance phase percentage of the gait cycle. The analytical expression was verified by numerical simulation and experimental, showing that the analytical estimation had an uncertainty of less than 20%. This paper provides an analytical expression to estimate the displacement accuracy along the down direction of INS aided by ZUPT and altimeter measurements.

References

[1] X. Yun, E. R. Bachmann, H. Moore, and J. Calusdian, "Self-contained position tracking of human movement using small inertial/magnetic sensor modules," in *IEEE International Conference on Robotics and Automation*, Rome, Italy, Apr. 10-14, 2007.

[2] A. R. Jimenez, F. Seco, C. Prieto, and J. Guevara, "A comparison of pedestrian dead-reckoning algorithms using a low-cost MEMS IMU," in *IEEE International Symposium on Intelligent Signal Processing*, Budapest, Hungary, Aug. 26-28, 2009.

[3] D. Titterton, J. L. Weston, and J. Weston, *Strapdown inertial navigation technology*. IET, 2004, vol. 17.

[4] Y. Wang, S. Askari, C.-S. Jao, and A. M. Shkel, "Directional ranging for enhanced performance of aided pedestrian inertial navigation," in *IEEE International Symposium on Inertial Sensors and Systems (INERTIAL)*, Naples, Florida, USA, Apr. 1-5, 2019.

[5] E. Foxlin, "Pedestrian tracking with shoe-mounted inertial sensors," *IEEE Computer graphics and applications*, no. 6, pp. 38–46, 2005.

[6] J.-O. Nilsson, A. K. Gupta, and P. Händel, "Foot-mounted inertial navigation made easy," in *International Conference on Indoor Positioning and Indoor Navigation (IPIN)*, Busan, Korea, Oct. 27-30, 2014.

[7] Y. Wang and A. M. Shkel, "Adaptive threshold for zero-velocity detector in ZUPT-aided pedestrian inertial navigation," *IEEE Sensors Letters*, vol. 3, no. 11, pp. 1–4, 2019.

[8] K. D. Rao, "Integration of GPS and baro-inertial loop aided strapdown INS and radar altimeter," *IETE Journal of Research*, vol. 43, no. 5, pp. 383–390, 1997.

[9] Y. Jiong, Z. Lei, D. Jiangping, S. Rong, and W. Jianyu, "GPS/SINS/BARO integrated navigation system for UAV," in *IEEE International Forum on Information Technology and Applications (IFITA)*, Kunming, China, Jul. 16-18, 2010.

[10] V. S. Sokolovic, G. Dikic, and R. Stancic, "Integration of INS, GPS, magnetometer and barometer for improving accuracy navigation of the vehicle," *Defense Science Journal*, vol. 63, no. 5, pp. 451–455, 2013.

[11] J. Zhang, E. Edwan, J. Zhou, W. Chai, and O. Loffeld, "Performance investigation of barometer aided GPS/MEMS-IMU integration," in *IEEE/ION Position, Location and Navigation Symposium*, Myrtle Beach, South Carolina USA, Apr. 23-26, 2012.

[12] A. Sabatini and V. Genovese, "A sensor fusion method for tracking vertical velocity and height based on inertial and barometric altimeter measurements," *Sensors*, vol. 14, no. 8, pp. 13 324–13 347, 2014.

[13] Z. Xinxi, Z. Rong, G. Meifeng, C. Gaofeng, N. Shulai, and L. Jinglong, "The performance impact evaluation on bias of gyro and accelerometer for foot-mounted INS," in *IEEE International Conference on Electronic Measurement & Instruments (ICEMI)*, Qingdao, China, Jul. 16-18, 2015.

[14] Y. Wang, A. Chernyshoff, and A. M. Shkel, "Error analysis of zupt-aided pedestrian inertial navigation," in *International Conference on Indoor Positioning and Indoor Navigation (IPIN)*, Nantes, France, Sep. 24-27, 2018.

[15] Y. Wang, D. Vatanparvar, A. Chernyshoff, and A. M. Shkel, "Analytical closed-form estimation of position error on ZUPT-augmented pedestrian inertial navigation," *IEEE Sensors Letters*, vol. 2, no. 4, pp. 1–4, 2018.

[16] Y. Wang, S. Askari, and A. M. Shkel, "Study on mounting position of imu for better accuracy of zupt-aided pedestrian inertial navigation," in *IEEE International Symposium on Inertial Sensors and Systems (INERTIAL)*, Naples, Florida, USA, Apr. 1-5, 2019.

[17] S. Askari, C.-S. Jao, Y. Wang, and A. M. Shkel, "A laboratory testbed for self-contained navigation," in *IEEE International Symposium on Inertial Sensors and Systems (INERTIAL)*, Naples, Florida, USA, Apr. 1-5, 2019.

Authorized licensed use limited to: Access paid by The UC Irvine Libraries. Downloaded on June 12,2020 at 03:58:13 UTC from IEEE Xplore. Restrictions apply.